Clays and Clay Minerals, Vol. 60, No. 6, 574–587, 2012.

STRUCTURES OF THE 2:1 LAYERS OF PYROPHYLLITE AND TALC

VICTOR A. DRITS[1], STEPHEN GUGGENHEIM[2], BELLA B. ZVIAGINA[1,*], AND TOSHIHIRO KOGURE[3]

[1] Geological Institute of the Russian Academy of Science, Pyzhevsky per. 7, 119017 Moscow, Russia
[2] Department of Earth and Environmental Sciences, University of Illinois at Chicago, Chicago, IL 60607, USA
[3] Department of Earth and Planetary Science, Graduate School of Science, The University of Tokyo, 7-3-1 Hongo, Bunkyo-ku, Tokyo, 113-0033, Japan

Abstract—To determine the relationships between the symmetry of the overall pyrophyllite and talc structure and the symmetry of individual layers, the geometry and symmetry of each 2:1 layer of pyrophyllite and talc were analyzed. For each, the previously published, refined unit cell may be rotated clockwise by ~60º for comparison to a layer unit cell. In pyrophyllite, the layer unit cell is ideal and shown to be orthogonal with *C*2/*m* symmetry. The agreement between the refined atomic coordinates and those calculated for the layer with *C*2/*m* symmetry confirms that the symmetry of the pyrophyllite layer is *C*2/*m*. The obliquity of the pyrophyllite refined cell results from the layer stacking and the choice of unit cell, but the interlayer stacking sequence does not disturb the layer symmetry. In contrast, talc has an oblique layer cell, without a mirror plane. For the most part, the distortion of the talc 2:1 layer is probably caused by an elongation of unshared O−O lateral edges around *M*1 that creates a slight corrugation of the octahedral sheet surface. Perhaps of lesser importance, the distortion of the talc layer cell may result from Coulombic interactions between cations of adjacent layers, and these cation-to-cation distances are sufficiently large (~6−7.5 Å) that the weak van der Waals forces that stabilize the stacking are not overcome. Because pyrophyllite has a vacant octahedral site, similar interactions are not present, and this results in a more idealized layer symmetry.

Phyllosilicates consisting of layers with an orthogonal cell and mirror plane (pyrophyllite, kaolinite, sudoite) were shown to have similar stacking faults. In these structures, the 2:1 or 1:1 layers have uniform orientation, and stacking faults occur owing to interstratifications of two alternative interlayer displacements in the same crystal that are related by a mirror plane in the projection on the (001) plane. In talc, stacking faults are associated with layer rotations by ±120º, whereas the lateral displacement between the adjacent tetrahedral sheets across the interlayer region is relatively ordered.

Key Words—Symmetry, Nature of Stacking Faults, Pyrophyllite, Talc, Unit-cell Parameters.

INTRODUCTION

Pyrophyllite, $Al_2Si_4O_{10}(OH)_2$, and talc, $Mg_3Si_4O_{10}(OH)_2$, are dioctahedral and trioctahedral varieties of layer silicates, respectively, and have several features in common. Both minerals have simple cation compositions with only minor isomorphous substitutions in the octahedral and tetrahedral sites; their layers are electro-neutral, and, in contrast to micas and smectites, the interlayer region contains neither cations nor H_2O molecules.

Zvyagin *et al.* (1969) deduced possible polytype modifications of talc and pyrophyllite. They described natural 1*A* talc and synthetic 2*M* pyrophyllite. In the symbolic notation of these authors, the idealized one-layer triclinic and two-layer monoclinic polytypes can be represented by the vector sequences of $\sigma_2\sigma_2\tau_1\sigma_2\sigma_2$ and $\sigma_2\sigma_2\tau_1\sigma_2\sigma_2\tau_5\sigma_2\sigma_2\tau_1$, respectively. Here, σ is the intralayer displacement in the (001) projection between the centers of the ditrigonal rings of the lower tetrahedral sheet and vacant *trans*-octahedra and between the centers of the *trans*-octahedra and ditrigonal rings of the upper tetrahedral sheets in a unit layer. The vector, τ, is the interlayer displacement between adjacent tetrahedral sheets across the interlayer (Guggenheim *et al.*, 2009). In the idealized structure, the fractional x and y components corresponding to σ_2 are ($a_o/6$, $-b_o/6$). The components of τ_1 are ($-a_o/6$, $-b_o/6$), where a_o and b_o are parameters of the idealized base-centered unit cell. According to Zvyagin *et al.* (1969), such interlayer displacements in pyrophyllite and talc minimize repulsive forces between the nearest tetrahedral cations and basal O atoms across the interlayer. For the one-layer polytype, the symbolic notation indicates that the unit cell of both minerals is rotated clockwise by 60º with respect to the idealized unit cell of the 2:1 layer with *C*2/*m* symmetry. For both minerals, the origin is in the center of the *trans* octahedron. In the idealized layer cell, the [100] direction coincides with the layer mirror plane. The combination of the intralayer and interlayer displacements, defined as "layer displacement" by Guggenheim *et al.* (2009), leads to triclinic symmetry of both structures having a monoclinic-shaped unit cell. Indeed, the intralayer displacement in the (001) plane is the sum of $\sigma_2 + \sigma_2 = 2(a_o/6 - b_o/6) = a_o/3 - b_o/3$. Thus,

* E-mail address of corresponding author:
zviagina@ginras.ru
DOI: 10.1346/CCMN.2012.0600603

the layer displacement on the (001) plane is $2\sigma_2 + \tau_1 = a_o/3 - b_o/3 - a_o/6 - b_o/6 = a_o/6 - b_o/2$, with the components $(-a_o/3, 0)$ taking into account the base-centered unit cell. Zvyagin *et al*. (1969) assumed that the one-layer polytype of both minerals has *C*1 symmetry.

Wardle and Brindley (1972) performed a partial refinement of a well crystallized natural pyrophyllite-1*A* from powder X-ray diffraction (XRD) data and confirmed the stacking sequence described by Zvyagin *et al.* (1969) for the one-layer polytype, albeit in $C\bar{1}$ symmetry. Later, Lee and Guggenheim (1981) performed a complete, single-crystal refinement of pyrophyllite-1*A*. Rayner and Brown (1973) and Drits *et al.* (1975) determined the crystal structure of talc from Weissenberg data and confirmed the one-layer structural model of Zvyagin *et al.* (1969) in $C\bar{1}$ symmetry. A precise, single-crystal refinement of talc by XRD was made by Perdikatsis and Burzlaff (1981).

A comprehensive review of pyrophyllite and talc structural and crystal-chemical features was presented by Evans and Guggenheim (1988). However, the relationship between the geometry and symmetry of the refinement results compared to the idealized layer unit cells was not considered. The aim of the present work was to consider further the nature of the cell with additional comparisons with the ideal 2:1 layer.

RESULTS

Transformation from the oblique to orthogonal unit cell of the layer

Two features in common for the refined unit-cell parameters of pyrophyllite and talc are: the angle γ is not equal to 90° and the ratio $b/a > \sqrt{3}$ (Tables 1, 2). These features are assumed to be interrelated and to result from the rotation of the refined unit cell with respect to the idealized orthogonal layer cell. Two possible oblique unit cells (cell 1 and cell 2) may be chosen in the two-dimensional lattice with an orthogonal unit cell having parameters a_o and b_o (Figure 1). Both oblique unit cells have the same *a* and *b* parameters, but differ in the orientation of their *a* and *b* axes with respect to those of the orthogonal cell. The distance between the ends of the *a* and *b* vectors of cell 1 is $2a$, whereas in cell 2 it is $2a_o$. The parameters of the orthogonal and oblique cells are interrelated (Figure 1):

$$4a^2 = a_o^2 + b_o^2;\ 4b^2 = b_o^2 + 9a_o^2, \text{ or } b^2 - a^2 = 2a_o^2 \qquad (1)$$

The a_o, b_o values can be determined from equation 1 if *a* and *b* are known and *vice versa*. The deviations of b/a and b_o/a_o from $\sqrt{3}$ are also interrelated because

$$b^2/a^2 = (9 + b_o^2/a_o^2) / (1 + b_o^2/a_o^2) \qquad (2)$$

Thus, if $b_o^2/a_o^2 < 3$, then $b^2/a^2 > 3$, and *vice versa*.

The difference between the two oblique cells is that for cell 1, the *a* axis is rotated clockwise by ~60° with respect to that of the orthogonal cell, and for cell 2, the *a* axis is rotated counterclockwise (Figure 1). In the refined structures of pyrophyllite (Lee and Guggenheim, 1981) and talc (Perdikatsis and Burzlaff, 1981), which correspond to cell 1, the *a* and *b* axes are rotated clockwise by ~60° with respect to the idealized unit cell of the layer (oriented such that a mirror plane or pseudo-mirror plane of the layer is parallel to the a_o axis).

Pyrophyllite. Consider the relationships between the parameters of the two-dimensional orthogonal cell and oblique cell 1. Figure 1 shows that $b_o/a_o = \tan\gamma_1$, $b_o/3a_o = \tan\gamma_2$, and $\gamma = \gamma_1 + \gamma_2$ is the angle between the *a* and *b* of cell 1.

If $b_o/a_o < \sqrt{3}$, then $\gamma_1 < 60°$, $\gamma_2 < 30°$, and $\gamma < 90°$; and, if $b_o/a_o > \sqrt{3}$, then $\gamma > 90°$. Figure 1 shows:

$$\sin\gamma_1 = b_o/2a;\ \cos\gamma_1 = a_o/2a \text{ and } \sin\gamma_2 = b_o/2b;\ \cos\gamma_2 = 3a_o/2b \qquad (3)$$

These relationships are valid for pyrophyllite where the 2:1 layers have orthogonal cells and the a_o axis coincides with the layer mirror plane. After application of equations 1–3, the refined oblique pyrophyllite unit-cell parameters (a = 5.160 Å, b = 8.966 Å, γ = 89.64°; Lee and Guggenheim, 1981) correspond also to the orthogonal layer cell with a_o = 5.1848 Å, b_o = 8.9230 Å, γ_o = 90°, and b_o/a_o = 1.721. Moreover, the sum of γ_1 and γ_2 calculated from the a_o and b_o parameters (equation 3) equals 89.68°, which is within two sigma of the experimental γ = 89.64(3)°. Thus, the structure of the pyrophyllite 2:1 layer is consistent with a two-dimensional orthogonal unit cell and a mirror plane.

Similar results are obtained from matrix algebra by using *CrystalMaker*® (2012) as a matrix multiplier. A constraint of *CrystalMaker*® is that identipoints may not be re-defined. Therefore, to obtain a nearly orthogonal cell, the pyrophyllite-1*A* asymmetric unit was expanded by removing the $C\bar{1}$ symmetry (cell 1, Figure 1) and then recast from a one-layer to a three-layer sequence such that the cell corners (identipoints) produce a pseudo-orthogonal cell (a = 5.16, b = 8.966, c = 27.57 Å, α = 91.13, β = 89.86, γ = 89.64 °). A 60° clockwise rotation was obtained by the transformation matrix of {½, ½, 0/ $-{}^3/_2$, ½, 0/ 0, 0, 1} and the origin adjusted to be on the mirror plane (a_o = 5.1848 Å, b_o = 8.9230, c_o = 27.57 Å, α = 90.69, β = 90.90, γ = 90.00°).

Talc. From equations 1 and 2, the refined unit cell of talc with a = 5.290Å, b = 9.173Å, γ = 90.09°, and b/a = 1.734 corresponds to an orthogonal unit cell with a_o = 5.2990 Å and b_o = 9.1573 Å (Tables 1,2). Because the refined and idealized layer cells in talc are rotated by ~60° as in pyrophyllite, the γ angle (equation 3) of the idealized cell is 89.886° and b_o^2/a_o^2 = 2.986. The refined γ value (Perdakatsis and Burzlaff, 1981), however, is 90.09(5)°, which differs from the calculated value by 4 sigma.

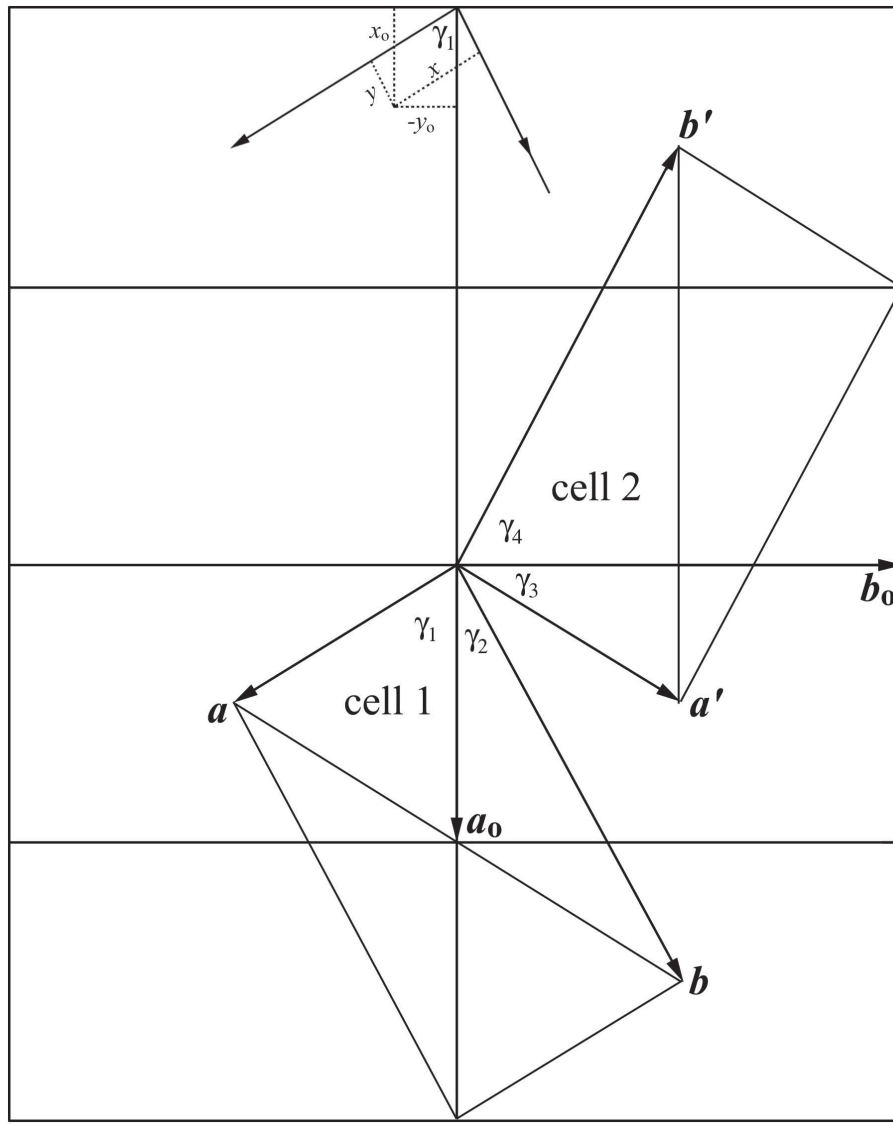

Figure 1. Oblique cells 1 and 2 having different orientations with respect to the orthogonal unit cell. Cells 1 and 2 are described by a, b, γ and a, b, γ' parameters, where $a = a'$, $b = b'$, and $\gamma \neq \gamma'$. γ_1 and γ_2 are the angles between a_o and a and b, respectively; γ_3 and γ_4 are the angles between b_o and a' and b', respectively.

As given above, another two-dimensional lattice with an orthogonal unit cell having $b_o^2/a_o^2 < 3$ is the oblique cell 2 for which $b^2/a^2 > 3$ and $\gamma > 90^o$. For the orthogonal unit cell with a_o and b_o, the following relationships are valid (Figure 1):

$$\tan \gamma_3 = a_o/b_o, \text{ with } \gamma_3 > 30^o$$
$$\text{and } \tan \gamma_4 = 3a_o/b_o, \text{ with } \gamma_4 > 60^o \quad (4)$$

so that, in the talc structure, the angle between the a and b axes of the oblique cell 2 is $\gamma = \gamma_3 + \gamma_4 = 90.114^o$. This value coincides, within error, with the refined $\gamma_{exp} = 90.09(5)^o$. Thus, in Figure 1, the refined unit cell of talc corresponds to cell 2. To maintain the relationships between the parameters of different unit cells that describe the same two-dimensional lattice, using $\gamma = 90.114^o$ is convenient. The mutual arrangement of the refined oblique and orthogonal cells in the talc structure, therefore, differs from pyrophyllite. The refined oblique cell of talc is rotated counterclockwise by 59.943° with respect to the orthogonal cell with a_o and b_o and clockwise by 60.114° with respect to the layer unit cell 1. The latter is also oblique with $a' = 5.290$ Å, $b' = 9.173$ Å, and $\gamma' = 89.886^o$ (Figure 2). Indeed, γ' is equal to the sum of $\gamma_1 = \arccos(b \cos 0.114^o/2b') = 60.00^o$ and $\gamma_2 = \arccos(b \cos 0.114^o/2a) = 29.886^o$ where $b \cos 0.114^o$ is the projection of the b parameter on the normal to the a axis.

Table 1. Refined unit-cell parameters.

Mineral	a (Å)	b (Å)	c (Å)	α (º)	β (º)	γ (º)	d_{001} (Å)	Reference
Pyrophyllite	5.160(2)	8.966(3)	9.347(6)	91.18(4)	100.46(4)	89.64(3)	9.1899	Wardle and Brindley (1972)
Talc	5.290(3)	9.173(5)	9.460(5)	90.46(5)	98.68(5)	90.09(5)	9.3514	Perdikatsis and Burzlaff (1981)

In summary, the talc two-dimensional layer lattice can be described by three cells: the refined oblique cell, the orthogonal cell rotated clockwise by 59.943º with respect to the refined cell, and an oblique cell with γ = 89.886º. The latter is rotated counterclockwise by 60.114º with respect to the refined cell and corresponds to the idealized layer unit cell (Figure 2; Table 2). In contrast to pyrophyllite, the idealized layer cell is deformed and the talc layer has no mirror plane.

Relationship between fractional atomic coordinates of the orthogonal and oblique layer unit cells

To reveal the relationship between fractional atomic coordinates of the orthogonal and oblique layer unit cells, the refined atomic coordinates were transformed from oblique to the orthogonal coordinate system of the structure. The coordinates of any point in the orthogonal cell, X_o, Y_o, Z_o, and oblique layer unit cell 1, *X, Y, Z*, are related by the equations (Figure 1):

$$\begin{aligned} X_o &= X \cos \gamma_1 + Y \cos \gamma_2 \\ Y_o &= -X \sin \gamma_1 + Y \sin \gamma_2 \\ Z_o &= Z \end{aligned} \quad (5)$$

From equations 3, the fractional Cartesian atomic coordinates of the orthogonal x_o, y_o and oblique x, y cells are related as:

$$\begin{aligned} x_o &= 0.5x + 1.5y \\ y_o &= -0.5x + 0.5y \\ z_o &= z \end{aligned} \quad (6)$$

Thus, the refined fractional Cartesian atomic coordinates of pyrophyllite are transformed into those of the orthogonal cell using the matrix:

$$\{½, ⅜, 0/-½, ½, 0/0, 0, 1\} \quad (7)$$

A similar procedure for talc shows that to transform the refined atomic coordinates into those of the oblique cell with a = 5.290 Å, b = 9.173 Å, γ = 89.884º and those of the orthogonal cell with a_o = 5.2990 Å and b_o = 9.1573 Å, the matrices {½, ⅜, 0/−½, ½, 0/0, 0, 1} and {½, −⅜, 0/½, ½, 0/0, 0, 1}, respectively, are used.

The atomic coordinates for the pyrophyllite orthogonal unit cell and the talc oblique cell with $C\bar{1}$ symmetry are given in Tables 3 and 4. The refined components of the layer displacements along the [100] and [010] directions are −0.3286a and −0.0202b for pyrophyllite and −0.2698a and −0.0085b for talc. The corresponding components of the layer displacements of the pyrophyllite orthogonal and talc oblique (γ = 89.884º) cells can be obtained using the same matrix that relates the fractional atomic coordinates of the refined oblique and orthogonal cells of pyrophyllite (Table 2).

DISCUSSION

Symmetry of the pyrophyllite 2:1 layer

A distinguishing feature of the atomic coordinates in the layer orthogonal unit cell in $C\bar{1}$ symmetry is pairs of atoms with nearly identical x and z coordinates and y coordinates of opposite sign and similar absolute values

Table 2. Parameters of the unit cells in the two-dimensional lattices of pyrophyllite and talc; *X* and *Y* are components of the layer displacements along the *a* and *b* axes, respectively.

Name of the cell	a (Å)	b (Å)	b/a	γ (º)	X	Y
Pyrophyllite						
Refined cell	5.160	8.966	1.738	89.68	−0.3286	−0.0202
Orthogonal layer cell	5.1848	8.9230	1.721	90.0	−0.1946	0.1542
Oblique cell 2	5.160	8.966	1.738	90.32	−0.1340	−0.1744
Talc						
Refined cell	5.290	9.173	1.734	90.114	−0.26985	−0.00849
Oblique layer cell	5.290	9.173	1.734	89.884	−0.14766	0.13068
Orthogonal cell	5.2990	9.1573	1.728	90.0	−0.12220	−0.13917

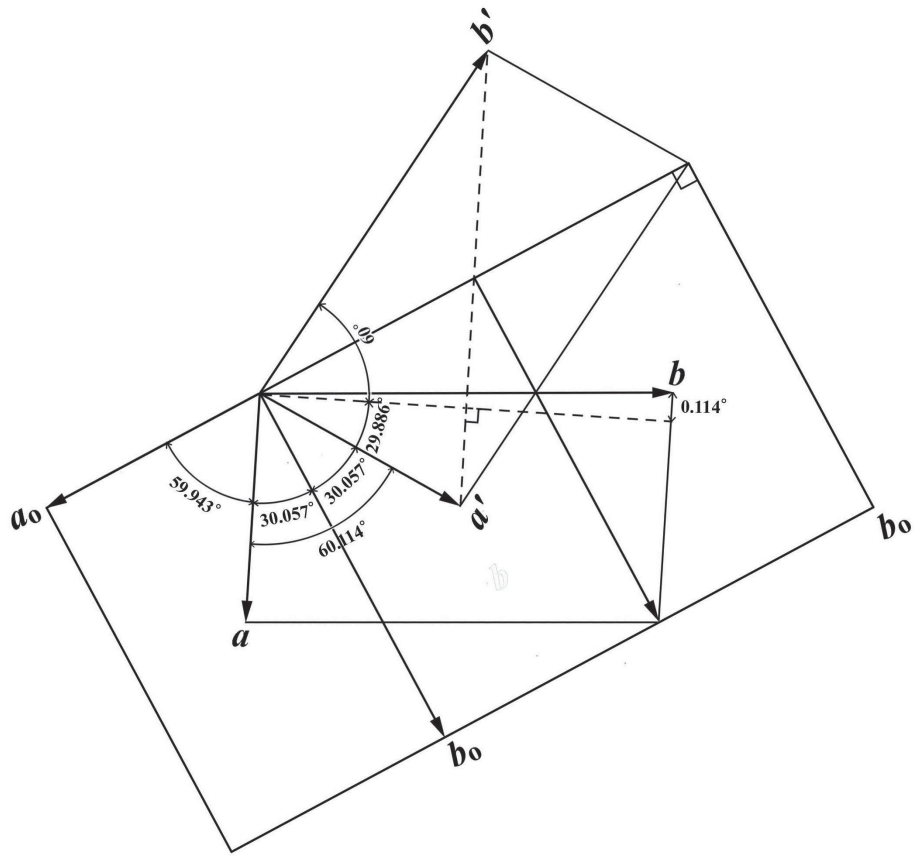

Figure 2. Mutual arrangement of the three-layer unit cells in the talc lattice: the refined oblique (a, b, γ = 90.114º), oblique conventional (a', b', γ = 89.886º) and orthogonal (a_o, b_o) cells.

(Table 3). This suggests that the symmetry of the pyrophyllite layer, without stacking considerations, is $C2/m$. To confirm this supposition, the values of x, y, z coordinates of these particular atomic pairs were averaged. Comparison of the coordinates of the same atoms obtained in terms of space groups $C\bar{1}$ and $C2/m$ for the layer (without considering stacking) shows that the differences in x vary from 0 to 0.0003; in y, from 0 to 0.0004; and in z, from 0 to 0.0003 (Table 3) around the average positions. For most atoms, these values are less than or equal to the experimental errors of the refined atomic coordinates. Thus, the values of the interatomic distances in the octahedral and tetrahedral sheets of the 2:1 layer for the refined structure coincide with those calculated using the atomic coordinates corresponding to the idealized $C2/m$ layer symmetry.

The relationship between the hk indices corresponding to the same structure factor, $F(hkl)$, as calculated in

Table 3. Comparison of the atomic coordinate in the orthogonal pyrophyllite layer unit cell in $C\bar{1}$ and $C2/m$ symmetry.

	—— $C\bar{1}$ symmetry ——			—— $C2/m$ symmetry ——			—— Differences ——		
	x	y	z	x	y	z	Δx	Δy	Δz
Al_1	0.500325	−0.16623	0	0.5	0.16623	0	0.00032	0	0
Si_1	0.811138	0.171009	0.29169	0.811328	0.171405	0.291995	0.00019	0.0004	0.00030
Si_2	0.311519	0.328203	0.2923	0.311328	0.328595	0.291995	0.00019	0.0004	0.0003
O_1	0.304972	−0.30604	0.1155	0.304993	−0.30604	0.11565	0.00002	0.00006	0.00015
O_2	0.805014	−0.1939	0.1158	0.804993	−0.19396	0.11565	0.00002	0.00006	0.00015
OH_1	0.381162	−0.00013	0.1081	0.381162	0	0.1081	0	0.00013	0
O_{b1}	0.538703	0.224987	0.3589	0.538527	0.22521	0.35865	0.00018	0.00022	0.00025
O_{b2}	0.53835	−0.22544	0.3584	0.538527	−0.22521	0.35865	0.00018	0.00023	0.00025
O_{b3}	0.871791	0.000034	0.3325	0.871791	0	0.3325	0	0.00003	0

Table 4. The actual and averaged atomic coordinates in the talc layer oblique conventional unit cell in $C\bar{1}$ symmetry.

	$C\bar{1}$ symmetry			Averaged			Differences		
	x	y	z	x	y	z	Δx	Δy	Δz
Mg_1	0	0	0	0	0	0	0	0	0
Mg_2	0.500049	0.166592	−0.00006	0.5	0.166592	0	0.000049	0	0.00006
Si_1	0.83356	0.166679	0.29093	0.833666	0.166828	0.291	0.000106	0.000149	0.00008
Si_2	0.333773	0.333023	0.29108	0.333666	0.333172	0.2910	0.000107	0.000149	0.00008
O_1	0.333785	0.333018	0.1176	0.33361	0.333025	0.1176	0.000175	0.000007	0
O_2	0.833435	0.166968	0.1176	0.83361	0.166975	0.1176	0.000175	0.000007	0
OH_1	0.332973	0.000086	0.1126	0.332973	0	0.1126	0	0.000086	0
O_{b1}	0.351598	0.499889	0.3481	0.351598	0.5	0.3481	0	0.000111	0
O_{b2}	0.574856	0.241009	0.3494	0.574855	0.24099	0.3489	0	0.00002	0.0005
O_{b3}	0.074854	0.259029	0.3484	0.074855	0.25901	0.3489	0	0.00002	0.0005
H	0.333024	0.001528	0.203						

the oblique unit cell (a = 5.160 Å, b = 8.966 Å, γ = 89.63º) and in the orthogonal cell (a_o = 5.1847 Å, b_o = 8.923 Å) follows from the equality:

$$hx + ky = h_o x_o + k_o y_o$$

Using matrix 7, it is easy to show that

$$h = 0.5(h_o - k_o)$$
$$k = 0.5(3h_o + k_o)$$

The calculation of structure factors showed perfect agreement between the refinement (Lee and Guggenheim, 1981) and the model for the 2:1 layer in $C2/m$ layer symmetry (Figure 3). The oblique cell of pyrophyllite is, therefore, the result of the choice of the unit cell based on the stacking, whereas the symmetry of the pyrophyllite 2:1 layer is $C2/m$ and the particular interlayer stacking sequence does not disturb the layer symmetry.

Description of pyrophyllite structure transformed to C2/m layer symmetry

Conventionally, the origin of the layer orthogonal cell is chosen at the center of the vacant octahedron and the a_o axis coincides, in the projection along the c^* axis, with the layer mirror plane. The structure of a pyrophyllite 2:1 layer, including displacement ellipsoids based on the three-layer, pseudo-orthogonal cell discussed above, is shown in Figure 4. As noted by Lee and Guggenheim (1981), the displacement ellipsoids were probably affected by the difficulties in obtaining a high-quality crystal for the analysis, and thus include uncertainties in the atomic coordinates, thermal effects,

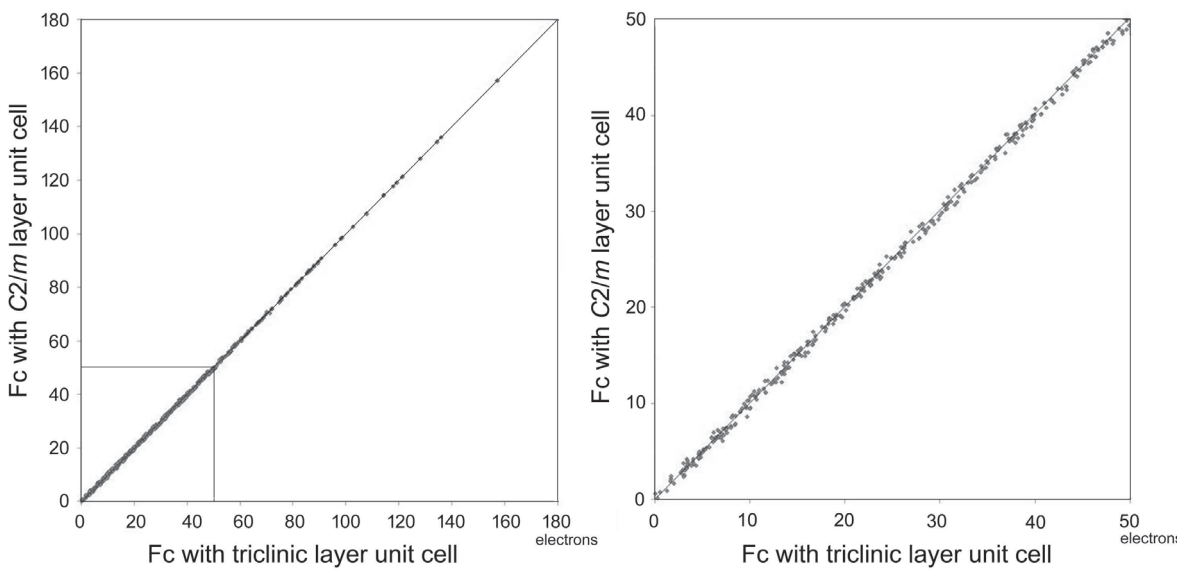

Figure 3. Structure factors (F_c) calculated using the conventional cell setting and atomic parameters reported by Lee and Guggenheim (1981) plotted against calculated structure factors using the new cell setting and 2:1 layer with $C2/m$ symmetry. The F_c values were calculated for 479 reflections with $d < 1.0$ Å. The diagram on the right is the magnified plot from the left diagram shown as a square.

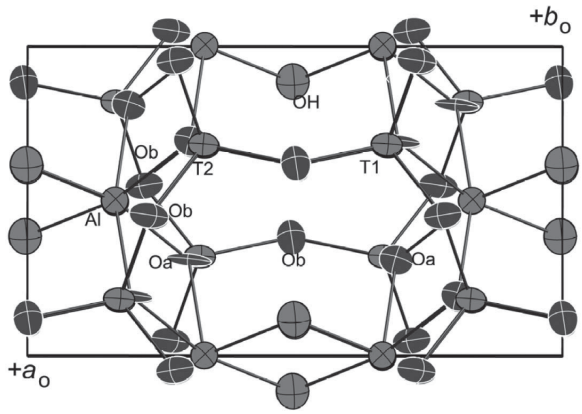

Figure 4. Pyrophyllite structure, with atom-displacement parameters, projected down the c_o axis of the pseudo-orthogonal cell described in the text. Systematic errors that may affect the displacement factors were described by Lee and Guggenheim (1981). Note that one of the two apical O atoms (Oa) is unreasonably disc shaped. The *C*2/*m* symmetry of the layer is consistent with the atom positions (see Table 3). For the most part, *C*2/*m* symmetry is approximated also by the displacement parameters. *T*1 and *T*2 indicate tetrahedral sites in $C\bar{1}$ symmetry. Oa = apical oxygen, Ob = basal oxygen (Figure produced using *CrystalMaker*®, 2012).

positional disorder, and any systematic errors in the data. The atomic coordinates are a more reliable indicator of symmetry than the displacement parameters. In general, however, the displacement parameters show consistency with *C*2/*m* symmetry.

The atomic coordinates (Table 3) allow calculation of the displacement of the center of the ditrigonal ring of the upper tetrahedral sheet with respect to the center of the vacant octahedron along the [100] direction, $\sigma_3 = 0.3163a_o$ (Figure 5). Similarly, the displacement of the center of the vacant octahedron with respect to the center of the lower tetrahedral sheet is also equal to $\sigma_3 = 0.3163a_o$ and the ring-to-ring centers displacement across the layer is $2\sigma_3 = 0.6326a_o$. The intralayer displacement, as measured across the pair of adjacent occupied *cis*-octahedra, is $(2\sigma_3 - a_o) = -0.3674a_o$. The components of the interlayer displacement, τ_2, which describes the displacement of the adjacent tetrahedral sheets across the interlayer, are $0.1728a_o$ and $0.1542b_o$. As a result, the components of the layer displacement, *t*, are $-0.1946a_o$ and $0.1542b_o$. Because the intralayer displacement coincides, in the (001) projection, with the layer mirror plane, the interlayer displacement can have two equally possible directions (τ_2 and τ_4) enantiomorphically related by the mirror plane (Figure 5). Each of these translations forms a one-layer triclinic pyrophyllite structure with the notation $\sigma_3\sigma_3\tau_2\sigma_3\sigma_3$ or $\sigma_3\sigma_3\tau_4\sigma_3\sigma_3$. These enantiomorphs of the 1*A* polytype are indistinguishable by diffraction methods. In contrast, their ordered stacking sequence results in a two-layer monoclinic 2*M* pyrophyllite structure with parameters a = 5.1848 Å, b = 8.9230 Å, c = 18.490 Å, $\beta = 96.26^o$ and the XRD pattern shown in Figure 6. The pattern is similar to that of Kogure *et al*. (2006a) who used a different approach to calculation.

The nature of stacking faults. The symmetrical arrangement of atoms with respect to the layer mirror plane in the pyrophyllite structure suggests a simple model for stacking faults. Because the interlayer displacement is described by the translation τ_2 ($0.1728a_0$, $0.1542b_0$), each successive layer in a periodic crystal is shifted, with respect to the preceding layer, by the same vector τ_2. A stacking fault occurs if a layer is shifted by τ_4 from an adjacent layer, in projection on (001), by a mirror

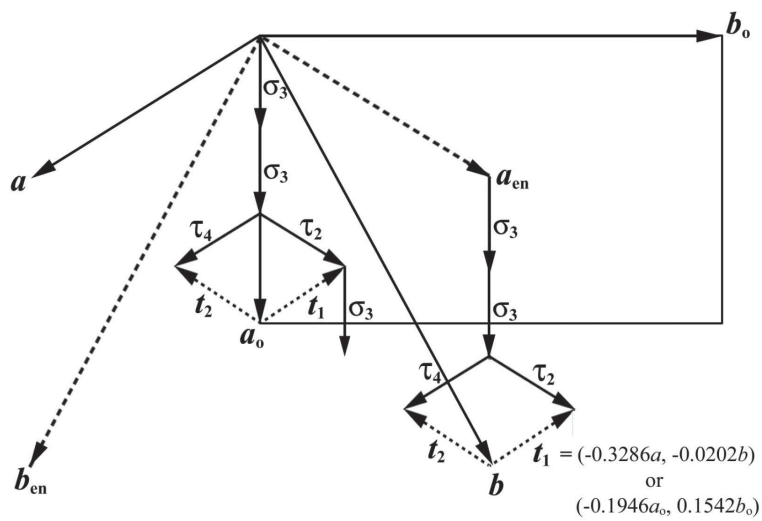

Figure 5. Relationships between the directions of the intralayer ($\sigma_3 + \sigma_3$), interlayer (τ_1, τ_2), and layer (t_1, t_2) displacements in the one-layer pyrophyllite structure, in which layers with *C*2/*m* symmetry have uniform orientation.

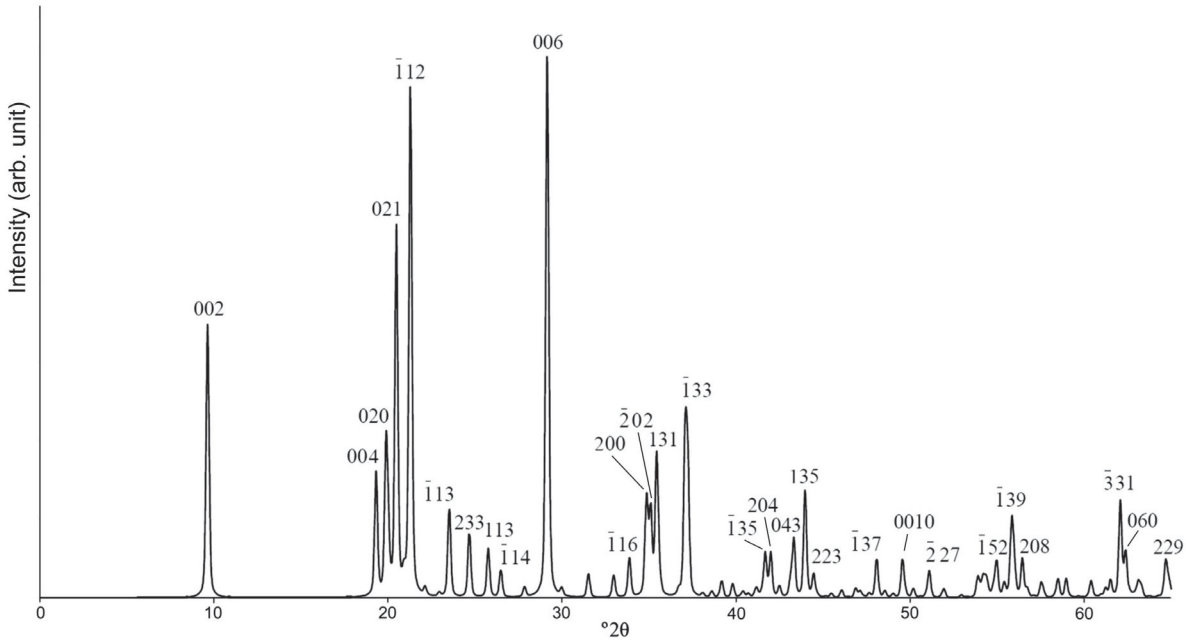

Figure 6. Powder XRD pattern calculated for the idealized 2*M* pyrophillite structure with parameters a = 5.1848 Å, b = 8.9230 Å, c = 18.490 Å, β = 96.26 º (CuKα1, λ = 1.5406 Å, full width at half-height of reflections + FWHH = 0.5).

plane or a glide plane that acts between these two layers (Figure 5). Both the periodicity and the cation arrangement in the 'defect' layer remain unaffected. Therefore, in the formation of such a layer, only minor changes occur in the potential energy of layer interaction. Thus τ_4 could be a new translation for a fragment between the 'defect' layer in question and the next stacking fault, where a τ_2 translation occurs. This defectless structural fragment is enantiomorphous with respect to the first one. Thus, stacking faults result from the intergrowth of right- and left-hand enantiomorphous pyrophyllite fragments described as the 2*M* polytype (Brindley and Wardle, 1970*)*.

Kogure *et al.* (2006a) studied stacking in pyrophyllite by high-resolution transmission electron microscopy (HRTEM) and found this stacking fault. Based on HRTEM images, the common stacking sequence is not the monoclinic cell with two-layer periodicity, but a uniform orientation of the 2:1 layers and near complete disorder of two interlayer displacements, *i.e.* lateral displacement between the two tetrahedral sheets across the interlayer. In fact, these interlayer displacements correspond to enantiomorphous choices as shown in Figure 5. Thus, the mirror plane in the pyrophyllite layer influences the nature of stacking faults in this mineral.

Layer silicates consisting of layers with a mirror plane have similar types of stacking faults owing to the probability of an equal occurrence for two alternative directions of interlayer displacement. Bookin *et al.* (1989) were the first to suggest this mechanism for stacking faults in kaolinite. They showed that the oblique cell of an ordered kaolinite with a = 5.153Å, b = 8.941Å, γ = 89.82º, as determined by Suitch and Young (1983), can be transformed into an orthogonal layer-based cell with a_o = 5.1666Å, b_o = 8.9174Å, γ = 90.00º. The observed γ value (89.82º) is equivalent to the γ value calculated by equation 3. In terms of the idealized model coordinate system (a, b, γ), the components of the layer translation t are ($-0.369a$, $-0.024b$). These components can be transformed into those in the orthogonal coordinate system (a_o, b_o) using matrix 7. The corresponding projection of the layer displacement is ($-0.2205a_o$, $0.1725b_o$). Because of the existence of the mirror plane, a different oblique cell can be chosen which is enantiomorphous with respect to the cell described above. That is, both cells have the same unit-cell parameters but the a, b axes are rotated either clockwise or counterclockwise with respect to those of the orthogonal cell. For the enantiomorphous cell, the layer displacement is ($-0.2205a_o$, $-0.1725b_o$). Bookin *et al.* (1989) predicted that the stacking faults in the kaolinite structure involve the interstratification of t_1 and t_2 layer translations with a uniform orientation of 1:1 layers. Plançon *et al.* (1989) showed by XRD, and Kogure and Inoue (2005) and Kogure *et al*. (2010) by TEM, that the stacking disorder is mainly caused by disorder of alternating t_1 and t_2 layer displacements, consistent with Bookin *et al*. (1989).

Sudoite, a di-trioctahedral chlorite (Kameda *et al.* , 2007) corresponding to a one-layer triclinic II*bb*-4 polytype, also shows a stacking sequence with a uniform layer orientation and with an intralayer displacement of $-a/3$ along the a axis. The interstratification involves two alternative layer displacements of similar magnitude

along directions rotated by ±60º with respect to the *a* axis.

These examples are consistent with the general conclusion that layer silicates consisting of layers that have an orthogonal cell and mirror planes have a similar set of stacking faults.

Talc

Cation interactions between layers and comparison to pyrophyllite. Although talc also has near end-member composition, the layer cell has a geometrical distortion. This distortion modifies the symmetry, giving it no mirror plane.

One of the causes of the layer cell distortions found in talc, but not in pyrophyllite, may involve stacking differences and the differences between dioctahedral *vs*. trioctahedral structures. In both talc and pyrophyllite, the tetrahedral sheets of two adjacent layers try to maintain the high-charge tetrahedral cations as far apart as possible and, thus, these cations are well shielded (Zvyagin *et al*., 1969). Hence, the layer stacking requires 'offset positioning' of the tetrahedra across the interlayer. This stacking is facilitated because neither pyrophyllite nor talc has an interlayer cation to help shield charges or to fix the tetrahedral ring of one layer directly above or below the tetrahedral ring of the adjacent layer.

The offset positioning of the layers, although it minimizes repulsive forces between the tetrahedral cations of adjacent layers, may not effectively minimize repulsive forces between other cations, especially those cations that are further apart or are of lesser charge than the tetrahedral cations. For example, octahedral cations of one layer may be poorly shielded with either tetrahedral cations, octahedral cations, or H^+ cations of an adjacent layer. If cation-to-cation distances are great, repulsive forces may be sufficiently minimized to prevent instability (by overcoming van der Waals forces that hold the layers together), but these repulsive forces may produce layer distortions.

Pyrophyllite and talc, projected down the *c* axis, are illustrated in Figure 7a and b, respectively. Each has three sheets projected: an (underlying) octahedral sheet of a lower layer (= layer 1), the upper tetrahedral sheet of layer 1, and the lower tetrahedral sheet of the next adjacent layer above layer 1 (= layer 2). For the lower tetrahedral sheet of layer 2 and the octahedral sheet of layer 1, the shielding effects involving *T*1 and *M*2, *T*1 and *M*1, and *T*1 and H for talc and the *T*1 and *M*2 for pyrophyllite (atoms labeled and designated as 'X' in Figure 7) are illustrated. *T*2 in talc is much better shielded than *T*1 because *T*2 superimposes over the bridging O atom of the underlying tetrahedra (in layer 1), and is not considered further. In contrast, *T*1 in talc overlies partially the vacant cavity (where an interlayer cation commonly resides in mica structures) and *T*1 can be affected by *M*2, H, or *M*1. The calculated distances (*d*) between relevant cations for talc are: $d(T1-M1)$ = 6.640 Å; $d(T1-M2)$ = 7.202 Å; and $d(T1-H)$ = 5.973 Å. The H^+ is poorly shielded relative to *T*1 (Si^{4+}) because the *T*1 tetrahedral basal edge is oriented between the *T*1 and H^+, which are relatively close (at 5.973 Å). *M*1 and *M*2 are further apart from *T*1, but both contain divalent (Mg) cations. Furthermore, projections down *c** (not shown) suggest that *M*1 and *T*1 are even more poorly shielded than illustrated in Figure 7. The combination of all these repulsive forces may act partially to distort the talc layer, but may not be sufficient to explain fully the layer distortions (see below).

For pyrophyllite, because *M*1 is vacant, the *M*2 site is the primary octahedral site that can interact with the *T*1 to produce repulsive forces; the relevant distance is $d(T1-M2)$ = 7.144 Å. However, the *M*2 cation is located (Figure 7a) in projection near a basal tetrahedral O atom, thereby partially shielding Si^{4+} from the Al^{3+} in the *M*2 site. As in talc, *T*2 is shielded partially from *M*2 because

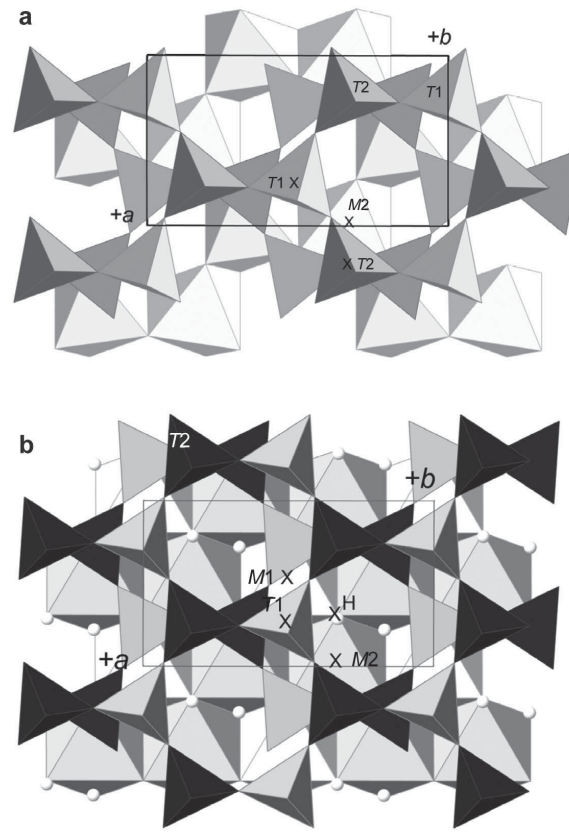

Figure 7. Polyhedral representation of portions of the crystal structure of (a) pyrophyllite and (b) talc projected down the *c* axis to illustrate shielding effects between selected cations. Each projection consists of an octahedral sheet and upper tetrahedral sheet (of layer 1) and the lower tetrahedral sheet of the next layer above (layer 2). The 'X' represents the cation location in projection as discussed in the text. In (b), the H atoms are represented by spheres.

of the association with a tetrahedral corner [$d(T2-M2)$ = 6.504 Å] and because $T2$ superimposes on a bridging O atom of the tetrahedral sheet in layer 1. Thus, repulsive forces are probably minimized adequately. However, unlike the talc structure (Perdikatsis and Burzlaff, 1981), the H position in pyrophyllite (Lee and Guggenheim, 1981) was not determined, although H positions have been determined for other Al-rich dioctahedral 2:1 phyllosilicates from neutron diffraction studies (*e.g.* Rothbauer, 1971 for muscovite). In muscovite, the O−H vector orientation is elevated by ~12º above the (001) plane and tilted away from the plane normal toward the vacant ($M1$) site. In pyrophyllite, the H elevation above the (001) may not be equal to muscovite with an interlayer cation; but, like muscovite, a H position can be obtained without the effect of repulsive forces from the vacant site. Thus, the repulsive forces between cations in adjacent layers are minimized in pyrophyllite. In contrast, the H position in talc is fixed by the Mg occupancy in $M1$ and $M2$ sites, and thus the O-H vector must point near the (001) plane normal, and toward the adjacent layer (layer 2).

However, the layer stacking and the interaction between layers in talc are probably not responsible for the reduced symmetry of the layer because the mutual arrangement of the $M1$, $M2$, and H sites should remain the same in talc layers that have either $C\bar{1}$ or $C2/m$ symmetry. Indeed, if the oblique cell with $\gamma = 90.09^{\circ}$ and $C\bar{1}$ is replaced by the cell with $\gamma = 90^{\circ}$ and $C2/m$ the distances $d(T1\text{-}M1)$, $d(T1\text{-}M2)$, and $d(T1\text{-H})$ do not change or changes will be negligible. However, the cation-to-cation interactions between the layers in talc probably are responsible for the lower symmetry of the overall unit cell that includes the effect of the layer stacking sequence.

Description of the structure and symmetry of the 2:1 layer. In talc, the refined atomic coordinates show high precision, which allows the determination of the H position. The atomic coordinates obtained in the coordinate systems of the refined and deformed layer cell are given in Table 4. Like pyrophyllite, the refined atomic coordinates of talc in $C\bar{1}$ symmetry are pairs of atoms with similar x and z coordinates and y coordinates of opposite sign and close absolute values. The differences between the x and y in these pairs vary from 0 to 0.0003, and the z coordinates of the basal O atoms show differences of 0.0005. Averaging of x, y, z coordinates of these atom pairs reduces the difference in the z coordinate of the basal O atoms significantly (Table 4), as expected. For most atoms, the averaged coordinates are within the experimental errors of the refined atomic coordinates.

The small differences observed between the pseudo-symmetry related atomic pairs (Table 4), however, likely provide an asymmetrical distribution of interatomic distances and contribute to the lack of a mirror plane in the idealized layer cell. Perdikatsis and Burzlaff (1981) showed that the *trans*- and *cis*-octahedra (Table 5) occupied by Mg have similar size and shape. In accord with the composition, the mean Mg−O, OH bond lengths are 2.071 Å for $M1$ and $M2$, and 2.070 Å for $M2'$ sites (Table 5). A significant feature of the octahedral sheet is the unshared lateral edges forming the upper triads of each octahedron (Figure 8). In the $M1$ octahedron the lateral edge O_1-O_2 (3.063 Å) is longer

Table 5. Selected octahedral and tetrahedral bond lengths (Å) in the upper part of the talc layer (from Perdikatsis and Burzlaff, 1981).

Distribution of Mg−O in $M1$, $M2$, and $M2'$ octahedra					
$M1-O_1$	2.082(1)	$M2-O_1$	2.076(1)	$M2'-O_1$	2.079(1)
$M1$−OH	2.052(1)	$M2$−OH	2.057(1)	$M2'$−OH	2.053(1)
$M1-O_2$	2.080(1)	$M2-O_2$	2.079(1)	$M2'-O_2$	2.078(1)
Mean	2.071	Mean	2.071	Mean	2.070
Unshared lateral edges:					
Triad edges, $M1$		Triad edges, $M2$		Triad edges, $M2'$	
O_1−OH	3.055(1)	O_1−OH	3.055(1)	O_1−OH	3.058(1)
O_1-O_2	3.063(1)	O_1-O_2	3.049(1)	O_1-O_2	3.058(1)
OH$-O_2$	3.053(1)	OH$-O_2$	3.062(1)	OH$-O_2$	3.054(1)
Mean	3.057	Mean	3.054	Mean	3.057
Distribution of Si−O in symmetrically independent tetrahedra					
Si_1-O_2	1.621(1)	Si_2-O_1	1.622(1)		
Si_1-O_{b3}	1.623(1)	Si_2-O_{b3}	1.624(1)		
Si_1-O_{b4}	1.623(1)	Si_2-O_{b4}	1.623(1)		
Si_1-O_{b5}	1.625(1)	Si_2-O_{b5}	1.621(1)		
Mean	1.623	Mean	1.623		

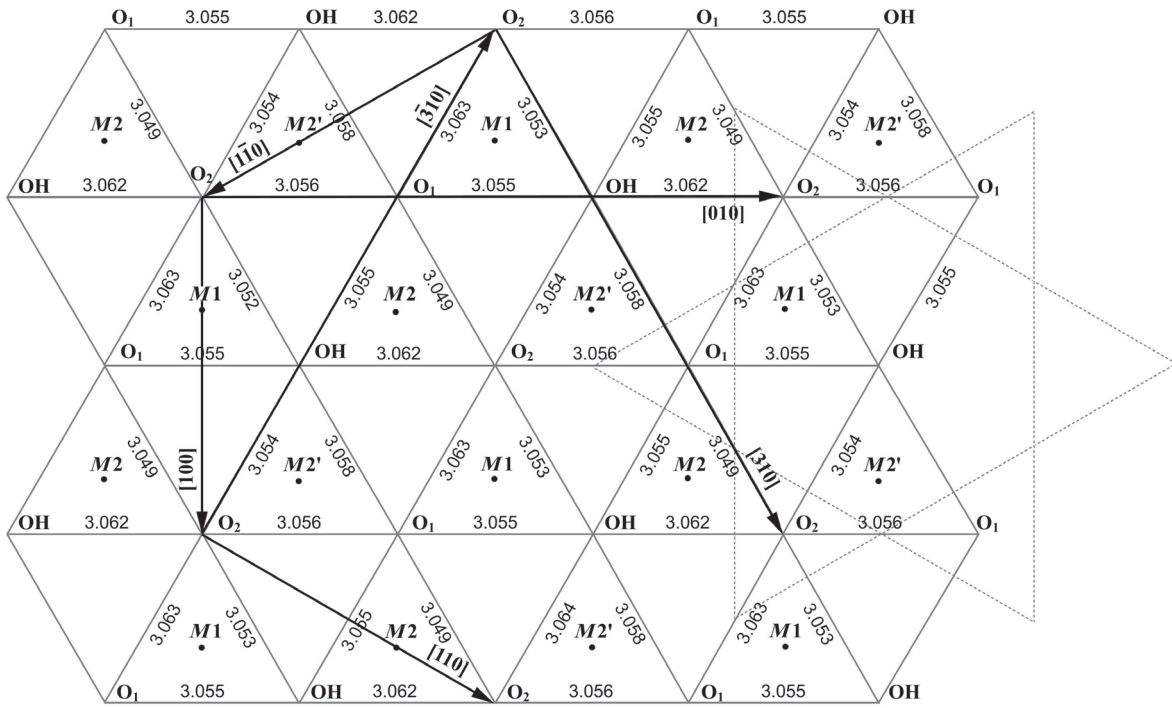

Figure 8. Distribution of the unshared lateral edges forming the upper surface of the octahedral sheet of the talc layer. The crystallographic directions corresponding to those of the three unit cells of the talc layer are shown (see also Figure 2). The dotted line shows traces of tetrahedral bases.

than O_1−OH (3.055 Å) and O_2−OH (3.053 Å). In contrast, in the *M*2 octahedron, the lateral edge O_1−O_2 (3.049 Å) is shorter than O_1−OH (3.055 Å), and O_2−OH (3.062 Å). In the *M*2′ octahedron, the edge lengths O_1−O_2 (3.056 Å), O_1−OH (3.058 Å), and O_2−OH (3.054 Å) have similar values.

The mean Si−O distances in symmetry-independent tetrahedra are equal to 1.623 Å, and this value is close to the individual Si−O bond lengths (Table 5). Because the lateral O_1−O_2 edge of the *trans*-octahedron (*M*1) is longer than those in the *cis*-octahedra (*M*2), the adjacent tetrahedra tilt across the elongated edge of this octahedron. Therefore, the corresponding bridging basal O atom moves within the layer by $\Delta z \approx 0.01$ Å. In contrast, because the unshared lateral O_1−O_2 edge of the *M*2 octahedron has the shortest length, the adjacent tetrahedra across this edge also tilt but the bridging O atom moves outside the layer by $\Delta z \approx 0.01$ Å. The basal surface of the tetrahedra is, therefore, slightly corrugated, producing three levels of the basal O positions along the *c** axis: one is slightly depressed within the layer, one is beyond the layer, and one is in between. The corrugation of the layer basal surface deduced from the lateral edges of the octahedral sheet is in agreement with the refined z coordinates of the basal O atoms (Table 4).

Although the observed variations in the interatomic distances are small, they probably play a crucial role in the reduction of symmetry in the layer structure. Consider the unshared lateral edges forming the upper surface of the octahedral sheet along [010], [310], and [3$\bar{1}$0] directions, as determined in the refined unit cell (Figure 8). The corrugation periods along [010] and [$\bar{3}$10] are close in value and equal to 9.173 Å (3.062 Å + 3.055 Å + 3.056 Å) and 9.172 Å (3.063 Å + 3.054 Å + 3.055 Å), respectively. In contrast, the period along [310] is significantly shorter and equal to 9.153 Å (3.049 Å + 3.053 Å + 3.058 Å). These values are equal to or close to those of $b = b' = 9.173$ Å and $b_0 = 9.157$ Å for the cells describing the two-dimensional lattice of the talc layer (Table 2, Figure 2). The observed difference between the calculated periods and the *b* parameters is related to the corrugation of the octahedral sheet surface owing to the depression of OH groups inside the sheet (Table 4) and to the differences in the individual unshared lateral edges along the three corrugation directions. Thus, the directions along [$\bar{3}$10] and [310] correspond to those of the b' and b_o axes of the oblique and orthogonal layer unit cells, respectively. The volume of the cells describing the same two-dimensional lattice is equal, indicating that the period along [1$\bar{1}$0] corresponding to the a_o parameter is longer than periods along [100] and [110] corresponding to a and a'. The unshared lateral edges show that the period along the [1$\bar{1}$0] is equal to the sum of the heights (2.652 Å + 2.646 Å) of two isosceles triangles with sides 3.0625 Å and 3.054 Å, respectively, and the angle between [1$\bar{1}$0] and [310] is 90.0°. Therefore, the [1$\bar{1}$0] and [310] directions corre-

spond to the orthogonal unit cell with a_o = 5.2990 Å and b_o = 9.1573 Å, as deduced from the refined unit-cell parameters (Table 2, Figure 2). Thus, the unshared lateral edge lengths on the upper surface of the octahedral sheet indicate that the two-dimensional layer lattice may be described by two other cells along with the refined cell: one orthogonal cell where the a_o axis along the [1$\bar{1}$0] is rotated clockwise by ~60º with respect to the refined cell, whereas the other cell has its a axis oriented along [110] and is rotated counter-clockwise by ~60º with respect to the refined cell (Figure 8). Thus, the periodicities and directions of the unit-cell edges correspond to the deformed layer and orthogonal cells deduced from the experimental values of the refined unit cell. In conclusion, the geometrical distortion of the layer unit cell occurs mostly because one of the unshared O–O lateral edges in each upper triad is elongated in *M*1 and shortened in the *M*2 octahedra.

Now consider a possible cause of these variations of the interatomic distances. Because talc does not have an interlayer cation and the O–H vector is 90º to the (001) plane, the H position is partly determined by the location of the nearest basal O atoms. The distances between the H and the basal O_{b1}, O_{b2}, and O_{b3} atoms are 2.888 Å, 2.887 Å, and 2.902Å, respectively (Perdikatsis and Burzlaff, 1981). Assuming that H contributes part of its positive charge to the basal O atoms, the O atom of the hydroxyl is under-saturated with respect to positive charge. Compensation occurs by the shortening of the Mg–OH bond to cause the depression of the O atom of the OH group within the octahedral sheets by Δz = 0.047 Å.

Furthermore, a small shift of each OH group towards the center of the *M*1 octahedron is observed. Small variations in the distances between OH and the nearest Mg cations are noted. Moreover, with Mg–OH distances shortening, the Mg–O bonds and O1–O2 lateral edge in the corresponding *M*1, *M*2, and *M*2′ octahedra (Figure 9) become larger. Thus, a local charge compensation of OH groups and O anions by Mg cations occurs owing to small shifts of these anions in the octahedral sheet of the layer. For example, the short Mg–OH = 2.052 Å and two longer Mg–O_1 = 2.081 Å and Mg–O_2 = 2.080 Å produce one long O_1–O_2 = 3.063(1) Å and two short O_1–OH = 3.055(1) Å and O_2–OH = 3.053(1) Å unshared lateral edges (Figure 9). The elongation of the O_1–O_2 edge requires small displacements of the O_1 and O_2. The elongation is shifted along [3$\bar{1}$0] and the displacements occur along [010] (Figure 8). These shifts redistribute the bond lengths of the *M*2 octahedron, shortening Mg–O_1 (2.076(1) Å) and the lateral O_1–O_2 edge (3.049(1) Å) and elongating Mg–OH (2.057(1) Å) and the unshared lateral O_2–OH edge (3.062(1) Å). The shifts of the O_1, O_2, and OH groups have no effect on the lateral unshared triad of the *M*2′ octahedron, and near equal Mg–O_1 and Mg–O_2 bonds form. Thus, the upper and lower surfaces of the octahedral sheet are related by a center of symmetry and the distortions are thereby identical. The observed distortions of the layer probably result from the redistribution of bond strengths owing to the interaction

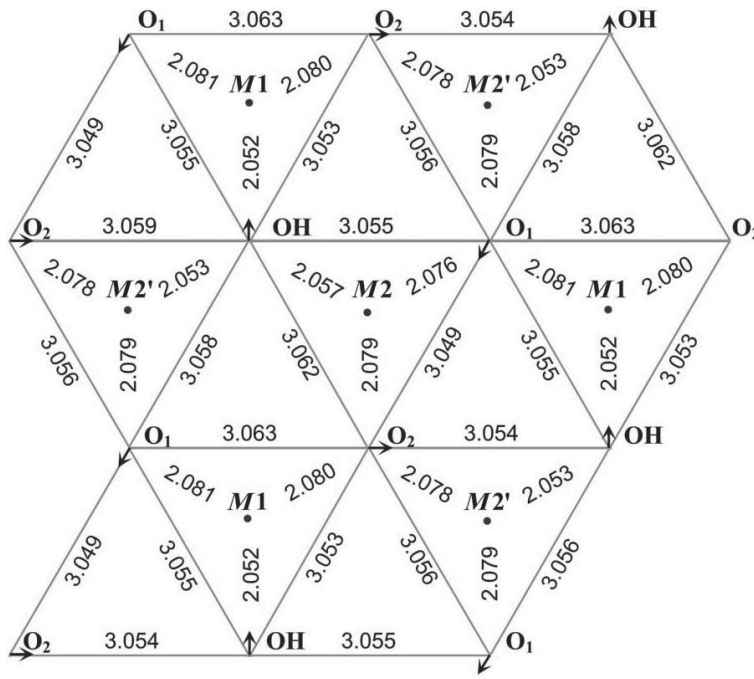

Figure 9. A fragment of the upper part of the octahedral sheet in the refined talc structure showing the distribution of individual *M*–O, O–O, and O–OH bond lengths in the *M*1, *M*2, and *M*2′ octahedra.

of the H atom and basal O atoms which are accompanied by the adjustments of the Mg–OH and Mg–O band lengths, and O–O lateral edges to provide a local charge balance of the O atoms of the octahedral sheet.

Stacking faults relating to layer rotation. One difference between pyrophyllite and talc (Kogure *et al.*, 2006a, 2006b) is that the 2:1 layers in pyrophyllite have the same orientation, and stacking faults occur at interstratification boundaries of two alternative interlayer displacements rotated with respect to each other by $\pm 2\pi/3$ (Figure 5). The fixed layer orientation regardless of the direction of the interlayer displacement probably causes the elongated, lath-shaped crystals as seen in pyrophyllite from Berezovsk (Kogure *et al.*, 2006a). In talc, three layer orientations occur, each rotated by ±120º with respect to each other. Lateral displacement between adjacent tetrahedral sheets across the interlayer region is relatively ordered. The observed regularities have been related (Kogure *et al.*, 2006a, 2006b) to the different surface corrugation of the basal surfaces of the tetrahedral sheets in pyrophyllite and talc layers. Because the vacant octahedra in pyrophyllite are larger than those occupied by Al, adjacent tetrahedra tilt across the elongated edges of these vacant octahedra and the corresponding bridging basal O atom moves within the layer by $\Delta z = 0.217$ Å, as compared to the other basal O atoms of each tetrahedron.

In contrast, in talc the basal O surface of the tetrahedral sheet is nearly planar because tetrahedra do not tilt around a larger vacant site. Kogure *et al.* (2008) suggested that the combination of a layer rotation and a surface corrugation is not favorable to stacking faults in the pyrophyllite structure. Because the surface corrugation is minimal in talc, stacking faults resulting from layer rotation do not depend on this effect. However, two factors do favor layer rotation in talc (Table 2). First, all layer orientations show *b*/*a* ratios that are nearly identical. Moreover, the *b*/*a* values are near 1.732, which is characteristic for a layer with hexagonal symmetry. Second, all the layer orientations have γ angles near 90º. Both factors favor stacking faults related to layer rotation. In contrast, the same two factors mentioned for talc are unfavorable for the pyrophyllite structure. In layers with different orientations the *b*/*a* ratios differ significantly from each other and from 1.732 (Table 2). In addition, the γ angles for two possible oblique cells deviate substantially from 90º. Therefore, in pyrophyllite, stacking faults due to layer rotation would be accompanied by significant incommensurability of the adjacent rotated layers. Kogure *et al.* (2006a) have reported that rotated layers are more common in a pyrophyllite specimen with fine grain size (Nohwa, South Korea). The observed fine grain size is probably due to incommensurability of the adjacent rotated layers.

CONCLUSIONS

Analysis of the refined unit-cell parameters and atomic coordinates of pyrophyllite (Lee and Guggenheim, 1981) showed that the 2:1 layer of pyrophyllite may be described as having an orthogonal unit cell (a_o = 5.1848 Å, b_o = 8.9230 Å) and *C*2/*m* symmetry, although the overall structure is $C\bar{1}$ when stacking symmetry is considered. The interlayer stacking sequence does not affect the layer symmetry. If displacement parameters are considered, which are affected by thermal motion, positional disorder, and errors in the refinement, the *C*2/*m* symmetry is equivocal. In this case, the displacement parameters can be shown to be an artifact of the relatively poor crystal quality used in the refinement. The pyrophyllite structure can alternatively be described using the atomic coordinates in the orthogonal unit cell with *C*2/*m* symmetry and the components $-0.1946a_o$ and $0.1542b_o$ of the layer displacement, *t*.

Phyllosilicates where layers can be described with an orthogonal unit cell and mirror plane, such as pyrophyllite, kaolinite, and sudoite, have stacking faults of nearly equal occurrence probability. These stacking faults have two alternative directions of the interlayer displacement related, in the projection on the *ab* plane, by the mirror plane of the layer.

Some distortions to the talc 2:1 layer may be related to Coulombic interactions between cations of adjacent layers. These interactions are weak because distances are relatively large, and they do not destabilize the talc structure; van der Waals forces are not overwhelmed by these interactions, but these interactions likely are also insufficient to fully distort the 2:1 layer from 2/*m* symmetry. The small corrugation of the octahedral sheet surface caused by the depression of the OH groups within the layer and the elongation of an unshared edge around *M*1 may be responsible for the distortions. In contrast, the repulsive forces between cations in adjacent layers in the pyrophyllite layer are better shielded than in talc, in part because of the vacant octahedral (*M*1) site in pyrophyllite. This vacancy eliminates a charged cation from interacting with adjacent layers in comparison to talc and allows for greater freedom for the H atom to minimize repulsions.

ACKNOWLEDGMENTS

V.A.D. and B.B.Z. are grateful to the Russian Foundation for Basic Research (grant 12-05-00381) for financial support.

REFERENCES

Bookin, A.S., Drits, V.A., Plançon, A., and Tchoubar, C. (1989) Stacking faults in kaolin-group minerals in the light of real structural features. *Clays and Clay Minerals*, **37**, 297–307.

Brindley, G.W. and Wardle, R. (1970) Monoclinic and triclinic

forms of pyrophyllite and pyrophyllite anhydride. *American Mineralogist*, **55**, 1259–1272.

CrystalMaker® (2012) *Interactive visualization for crystal and molecular structures*. Version 2.5.5, CrystalMaker Software Ltd, Oxford, England.

Drits, V.A., Aleksandrova, V.A., and Smolin, P.P. (1975) Refinement of the crystal structure of talc. P. 99–105 in: *Crystal Chemistry of Minerals and Geological Problems* (A.G. Kossovskaya, editor), Nauka, Moscow (in Russian).

Evans, B.W. and Guggenheim, S. (1988) Talc, pyrophyllite, and related minerals. Pp. 225–294 in: *Hydrous Phyllosilicates Exclusive of Micas* (S.W. Bailey, editor). Reviews in Mineralogy, **19**, Mineralogical Society of America.

Guggenheim, S., Adams, J.M., Bergaya, F., Brigatti, M.F., Drits, V.A., Formoso, M.L.L., Galán, E., Kogure, T., Stanjek, H., and Stucki, J.W. (2009) Nomenclature for stacking in phyllosilicates: Report of the Association Internationale pour l'Etude des Argiles (AIPEA) Nomenclature Committee for 2008. *Clay Minerals*, **44**, 157–159.

Kameda, J., Miyawaki, R., Kitagawa, R., and Kogure, T. (2007) XRD and HRTEM analyses of stacking structures in sudoite, di-trioctahedral chlorite. *American Mineralogist*, **92**, 1586–1592.

Kogure, T. and Inoue, A. (2005) Determination of defect structures in kaolin minerals by high-resolution transmission electron microscopy (HRTEM). *American Mineralogist*, **90**, 85–89.

Kogure, T., Jige, M., Kamdeda, J., Yamgishi, A., Miyawaki, R., and Kitagawa, R. (2006a) Stacking structures in pyrophyllite revealed by high resolution transmission electron microscopy (HRTEM). *American Mineralogist*, **91**, 1293–1299.

Kogure, T., Kameda, J., Matsui, T., and Miyawaki, R. (2006b) Stacking structure in disordered talc: Interpretation of its X-ray diffraction pattern by using pattern simulation and high-resolution transmission electron microscopy. *American Mineralogist*, **91**, 1363–1370.

Kogure, T., Kameda, J., and Drits, V.A. (2008) Stacking faults with 180º layer rotation in celadonite, iron and magnesium-rich dioctahedral mica. *Clays and Clay Minerals*, **56**, 612–621.

Kogure, T., Elzea-Kogel, J., Johnston, C.T., and Bish, D.L. (2010) Stacking disorder in a sedimentary kaolinite. *Clays and Clay Minerals*, **58**, 62–71.

Lee, J.H. and Guggenheim, S. (1981) Single crystal X-ray refinement of pyrophyllite-1Tc. *American Mineralogist*, **66**, 350–357.

Perdikatsis, B. and Burzlaff, H. (1981) Structurverfeinerung am Talk $Mg_3[(OH)_2Si_4O_{10}]$. *Zeitschrift für Kristallographie*, **156**, 177–186.

Plançon, A., Giese, R.F., Drits, V.A., and Bookin, A.S. (1989) Stacking faults in the kaolin-group minerals – defect structures of kaolinite. *Clays and Clay Minerals*, **37**, 203–210.

Rayner, J.H. and Brown, G. (1973) Structure of talc. *Clays and Clay Minerals*, **21**, 103–114.

Rothbauer, R. (1971) Untersuchung eines 2M1-Muskovits mit Neutronenstrahlen. *Neues Jahrbuch für Mineralogie Monatshefte*, 143–154.

Suitch, P.R. and Young, R.A. (1983) Atom positions in highly ordered kaolinite. *Clays and Clay Minerals*, **31**, 357–366.

Wardle, R. and Brindley, G.W. (1972) The crystal structure of pyrophyllite, 1Tc, and its dehydroxylate. *American Mineralogist*, **57**, 732–750.

Zvyagin, B.B., Mishchenko, K.S., and Soboleva, S.V. (1969) Structure of pyrophyllite and talc in relation to the polytypes of mica-type minerals. *Soviet Physics/Crystallography*, **13**, 511–515.

(*Received 18 May 2012; revised 20 October 2012; Ms. 673; AE: W.F. Jaynes*)